JPE 16-3-36

http://dx.doi.org/10.6113/JPE.2016.16.3.1200
ISSN(Print): 1598-2092 / ISSN(Online): 2093-4718

The Characteristics of Planar EMI Filter with Bi-Ground Layers Considering Impedance Mismatching

Shishang Wang†, Zheng Song*, and Qianceng Lou*

†,*Jiangsu Key Laboratory of New Energy Generation and Power Conversion, Nanjing University of Aeronautics and Astronautics, Nanjing, China

Abstract

Planar electromagnetic interference (EMI) filter has significant engineering significance to power electronic system integration and miniaturization. However, the value of differential mode capacitance cannot meet the demand of noise suppression because of the size limit of ceramics. In this case, the EMI filter of novel multilayers is recommended to address this issue. A novel integrated structure of EMI filter based on multilayer ceramic is proposed in this study. The inductance and capacitance of the new structure can be designed separately, which is an advantage in manufacturing. Insertion loss is measured more closely to the actual situation in this study, which is different from the condition where source and load impedances are both 50 Ω. In the process of designing a novel EMI filter, noise impedance is considered. Moreover, the prototype is created and applied to a small switching power supply, which verifies the effectiveness of the developed EMI filter.

Key words: Impedance mismatching, Multilayer ceramic capacitor, Planar EMI filter

I. INTRODUCTION

As switching frequency increases, the problem of electromagnetic interference (EMI) worsens and seriously affects the operation of the equipment. To meet the electromagnetic compatibility (EMC) standards, the planar EMI filter is extensively adopted for converters because of its small size, high power density, and small parasitic parameters [1], [2].

The traditional planar EMI filter is usually used to filter interference in switching power supplies and consists of inductor-capacitor (LC) units and *differential mode* (DM) capacitor, as shown in Fig. 1 [3]. The basic structure of the traditional planar EMI filter can be decoupled into two parts, namely, the DM filter and the *common mode* (CM) filter, which filter DM and CM interferences, respectively. In addition, one layer is connected to the ground for this type of EMI filter. Therefore, this filter structure is also called the *planar* EMI *filter* with *single ground layer* (PFSGL) in this study.

Of all the components in the integrated EMI filter, the LC unit (4, 6) and integrated DM capacitor (1, 9) are the most important functioning parts. The LC unit provides CM inductance and CM capacitance, where additional copper foil windings are added to increase CM inductances. The integrated DM capacitor mainly provides DM capacitance. Essentially, the integrated DM capacitor is also a basic LC unit, in which spiral multiple windings are replaced by one-turn winding to increase capacitance. The leakage inductance layer (5) is added to increase leakage inductance and provide DM inductance.

With all the required functioning parts, a complete EMI filter can be achieved with proper interconnection; its equivalent circuit schematic is illustrated in Fig. 2. The port of one DM capacitor (1) can be used as the input port of the EMI filter, whereas the port of other DM capacitors (9) can be used as the output port.

For the sake of technology, the number of helixes on both sides of the ceramic substrate is small, which is a problem because it cannot meet the requirements of inductance [4], [5]. At the same time, complete symmetry cannot be guaranteed in

Manuscript received Jun. 15, 2015; accepted Dec. 11, 2015
Recommended for publication by Associate Editor Jung-Wook Roh.
†Corresponding Author: wss.xjtu@163.com
Tel.: +86-13770755953, Nanjing Univ. of Aeronautics and Astronautics
*Jiangsu Key Laboratory of New Energy Generation and Power Conversion, Nanjing University of Aeronautics and Astronautics, China

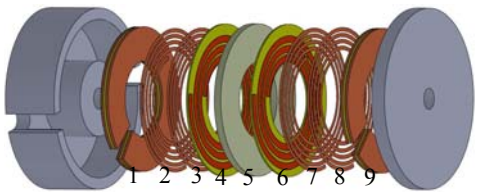

Fig. 1. The PFSGL.

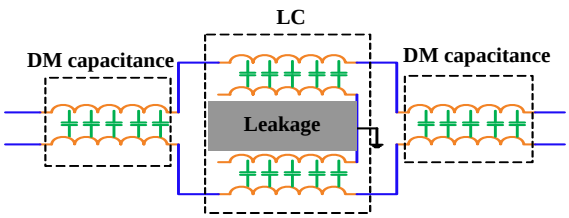

Fig. 2. The equivalent circuit schematic of the integrated EMI filter.

the LC unit. A *coupling* relationship exists between CM and DM noise, which causes certain errors, thus affecting the filtering effect of EMI filters. In addition, material and production process of planar EMI filters are also the main issues in filter implementation.

Several kinds of integrated EMI filters have been investigated in previous studies [6]-[8], which can improve the high-frequency characteristics and attenuate the noise effectively. With regard to the characteristics of impedance that varied with frequency, CM and DM noise are characterized by different source and load impedances [9], [10]. According to the impedance mismatch criteria, different types of EMI filters should be employed to suppress DM and CM noise.

Therefore, this study aims to present a novel *planar* EMI *filter* with *bi-ground layers* (PFBGL) and take CM noise as an example on how to select filter types. Compared with the PFSGL, improvement of the novel structure of the EMI filter has been proposed. Equivalent circuits of different types of filters are also proposed, which illustrate whether C-L or L-C filter is more suitable for the high source impedance condition.

II. Planar EMI Filter with Bi-Ground Layers

As mentioned previously, available studies on planar EMI filter are mainly focused on PFSGL. However, this study proposes a novel structure of the PFBGL (Fig. 3), which is composed of three parts, namely, L-unit, C-unit integrated CM capacitance, and DM capacitance single DM capacitance. Compared with the PFSGL, the PFBGL can easily achieve the decoupling design of inductance and capacitance.

For the PFBGL, the C-unit is composed of the silver layers (3, 5), copper layers (1, 7), and dielectric layers (2, 4, 6), which integrate CM and DM capacitance. Specifically, CM capacitance is achieved in the silver layers (3, 5) and copper layers (1, 7) under the CM excitation condition in parts 3 and 5 shown in Fig. 4. DM capacitance can be obtained in parts 3 and

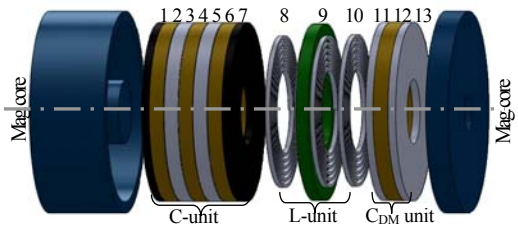

Fig. 3. The PFBGL.

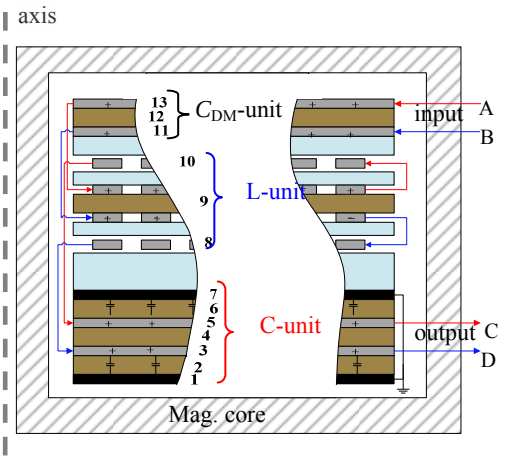

(a) L-C type.

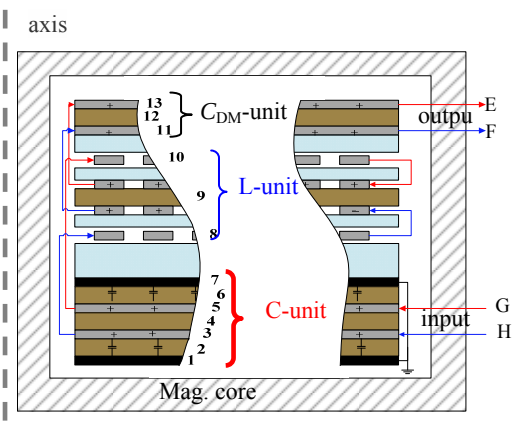

(b) C-L type.

Fig. 4. Linking of the CM filter.

5 under DM excitation of the two ports and the independent DM capacitance unit (11, 12, 13), respectively. More importantly, the high-permittivity ceramic substrate (2, 4, 6) must be selected for the C-unit and DM capacitance unit to ensure a large capacitance. In addition, the L-unit includes the main coil (9) and auxiliary coil (8, 10). CM inductance mainly occurs in the main coil because it has more turns and its wires are in the same direction. By contrast, auxiliary coils are only used to adjust DM inductance because its wires are in the opposite direction.

A. Under the CM Excitation Condition

The CM filter has two commonly used types of structures, namely, C-L type and L-C type, which refer to the filtering

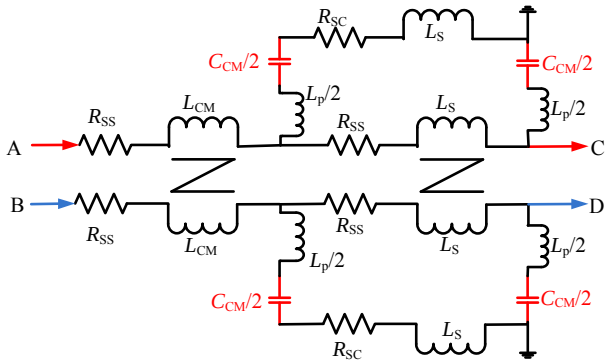

(a) L-C type.

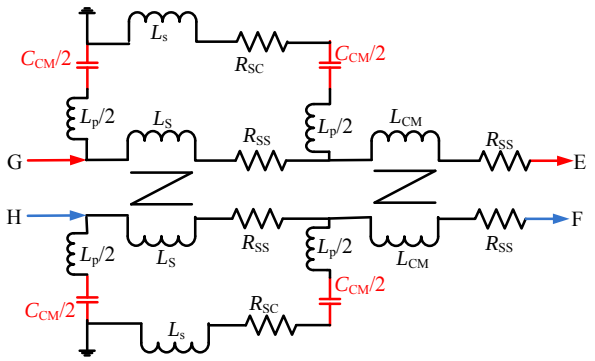

(b) C-L type.

Fig. 5. Lumped parameter model under CM excitation: R_{SS}, surface resistance of the silver layer; L_{CM}, inductance from the main coil; L_S, inductance from a single-turn metal (silver and copper); L_p, parasitic inductance of CM capacitance; R_{SC}, surface resistance of the copper layer; C_{CM}, CM capacitance from the silver layer to the ground.

capacitance and inductance close to the noise source with filter in the real circuit, respectively. Specifically, when the noise current flows into the C_{DM}-unit (11, 13) and flows out of the C-unit (3, 5), no capacitance effect occurs in the C_{DM}-unit and in the main coil (9) because the units are assumed completely symmetrical and the potential of both sides are the same. When applying CM excitation to the C-unit, parts 3 and 5 have the same capabilities and no potential difference exists between these two layers. However, given that parts 1 and 7 of the copper later are connected to the ground, a potential difference exists between the silver layer (3, 5) and the copper layer (1, 7), which provides the needed capacitance for the CM filter. This explains why the filter is called PFBGL.

In addition, when CM excitation is applied to the L-unit, magnetic fluxes from the main coil (9) can be mutually enhanced; however, fluxes from the two auxiliary (8, 10) coils cancel out. Therefore, CM inductance is only generated by the main coils, which provide the needed inductance for the CM filter.

Fig. 4 shows the linkages of the CM filter and the corresponding equivalent models to describe the corresponding functions of its parts.

According to our research, the C-L type should be selected when CM noise is characterized by high source and low load impedance. By contrast, the L-C type should be selected when CM noise is characterized by low source and high load impedance.

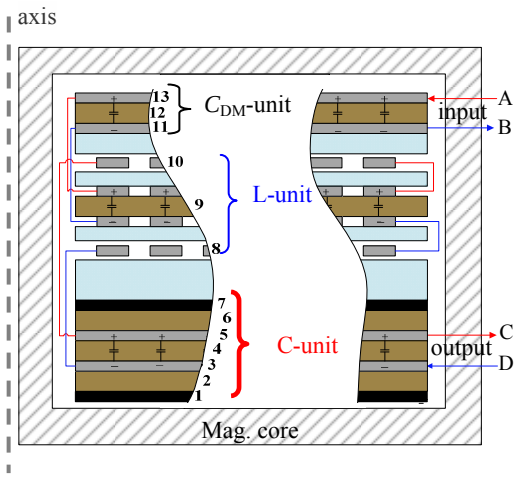

Fig. 6. C-L-C linking of the DM filter.

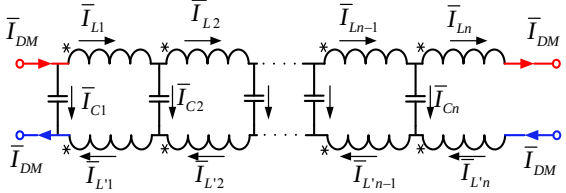

Fig. 7. Distribution parameter circuit.

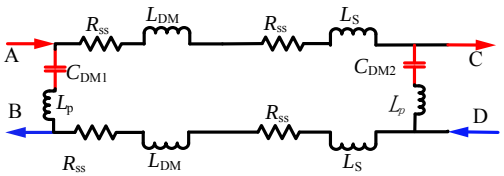

Fig. 8. Lumped parameter circuit under DM excitation: R_{SS}, surface resistance of the silver layer; L_{DM}, leakage inductance from the main coil; L_S inductance from a single-turn metal (silver and copper); L_p, parasitic inductance of CM capacitance; C_{DM1} and C_{DM2}, DM capacitance between silver layers.

B. Under the Condition of DM Excitation

The DM filter also has two types, namely, C-L-C and L-C-L, which refer to the filtering capacitance and inductance close to the noise source with the filter in the real circuit, respectively. The difference between these two types is relatively significant; thus, we select the C-L-C type in the following analyses. Fig. 6 shows a C-L-C type DM filter. Specifically, when DM current flows into the ports A and D and flows out of ports B and C (Fig. 6), a capacitance effect is observed in the C_{DM}-unit (11, 13) and C-unit (3, 5) because the potential of the two sides of the units is different. A capacitance effect is also observed in the main coil of the L-unit (9). However, the capacitance value is relatively small that it is usually ignored. In addition, DM inductance is often provided by the leakage inductance of CM

inductance.

Fig. 7 shows the distribution parameter circuit when DM excitation is applied to the L-unit (9), according to transmission line theory.

According to Kirchhoff's current law, the current of any inductance is expressed as follows:

$$\begin{bmatrix} \bar{I}_{L1} \\ \bar{I}_{L2} \\ \vdots \\ \bar{I}_{Ln} \end{bmatrix} = \begin{bmatrix} \bar{I}_{L'1} \\ \bar{I}_{L'2} \\ \vdots \\ \bar{I}_{L'n} \end{bmatrix} = \begin{bmatrix} \bar{I}_{DM} - \bar{I}_{C1} \\ \bar{I}_{DM} - (\bar{I}_{C1} + \bar{I}_{C2}) \\ \vdots \\ \bar{I}_{DM} - \sum_{j=1}^{n} \bar{I}_{Cj} \end{bmatrix}. \quad (1)$$

According to Kirchhoff's voltage law, the voltage of any inductance is expressed as follows:

$$\begin{bmatrix} \bar{E}_{L1} \\ \bar{E}_{L2} \\ \vdots \\ \bar{E}_{Ln} \end{bmatrix} = \begin{bmatrix} L_1 \frac{d\bar{I}_{L1}}{dt} + M\sum_{j=2}^{n} \frac{d\bar{I}_{Lj}}{dt} - M\sum_{j=1}^{n} \frac{d\bar{I}_{L'j}}{dt} \\ L_2 \frac{d\bar{I}_{L2}}{dt} + M\sum_{j=1}^{n} \frac{d\bar{I}_{Lj}}{dt} - M\sum_{J=1}^{n} \frac{d\bar{I}_{L'j}}{dt} - M\frac{d\bar{I}_{L2}}{dt} \\ \vdots \\ L_n \frac{d\bar{I}_{Ln}}{dt} + M\sum_{j=1}^{n-1} \frac{d\bar{I}_{Lj}}{dt} - M\sum_{j=1}^{n} \frac{d\bar{I}_{L'j}}{dt} \end{bmatrix}, \quad (2)$$

where M is the mutual inductance between any two small units. In Fig. 7, the values of self-inductance and mutual inductance of the small units are the same because of the existence of a closed magnetic core, namely, $M = L_i$ (i = 1, 2, …, n).

$$\begin{bmatrix} L_1(\frac{d\bar{I}_{L1}}{dt} + \sum_{j=2}^{n} \frac{d\bar{I}_{Lj}}{dt} - \sum_{j=1}^{n} \frac{d\bar{I}_{L'j}}{dt}) \\ L_2(\frac{d\bar{I}_{L2}}{dt} + \sum_{j=1}^{n} \frac{d\bar{I}_{Lj}}{dt} - \sum_{j=1}^{n} \frac{d\bar{I}_{L'j}}{dt} - \frac{d\bar{I}_{L2}}{dt}) \\ \vdots \\ L_n(\frac{d\bar{I}_{Ln}}{dt} + \sum_{j=1}^{n-1} \frac{d\bar{I}_{Lj}}{dt} - \sum_{J=1}^{n} \frac{d\bar{I}_{L'j}}{dt}) \end{bmatrix} = \begin{bmatrix} 0 \\ 0 \\ \vdots \\ 0 \end{bmatrix} \quad (3)$$

From Equation (3), the C-unit (1–7) and C_{DM}-unit can be equivalent to the capacitance under the condition of DM excitation, given that the induced electromotive force of any inductance is zero. Therefore, the equivalent lumped parameter circuit of the DM filter can be shown in Fig. 8.

Based on the previously presented analysis, the C-unit and DM capacitor are equivalent to one capacitor. Therefore, DM inductance can be produced by independent spiral wires. Moreover, DM capacitance C_{DM1} is generated between two silver layers of integrated capacitance and C_{DM2} denotes the capacitance of the C-unit.

C. Improvement of DM Capacitance

One of the main factors restricting the development of EMI filter miniaturization is its inability to achieve a large DM capacitance. Therefore, multilayer ceramic capacitors, which can increase DM capacitance to meet the design requirements, are proposed in this paper. Fig. 9 shows the capacitance unit,

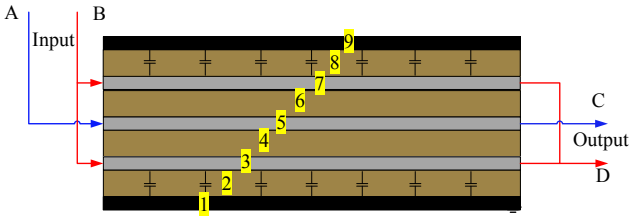

(a) CM.

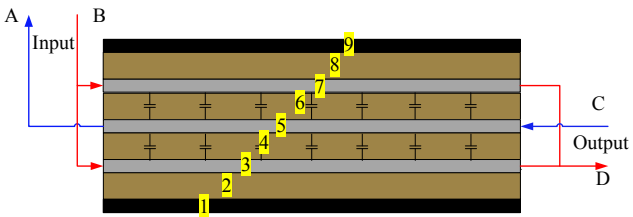

(b) DM.

Fig. 9. Linkage of the multilayer ceramic capacitors.

which is composed of multilayer ceramic.

As shown in Fig. 9, the C-unit is composed of the silver layers (3, 5, 7), copper layers (1, 9), and dielectric layers (2, 4, 6, 8), which integrate CM and DM capacitance. When CM current flows into the C-unit, the electric potential of the three silver layers is the same, and no capacitance exists between the silver layers. CM capacitance is still achieved between the silver and copper layers, and its value is unchanged. When DM current flows into the C-unit, DM capacitance between the silver layers increases because two capacitors exist in parallel.

III. Design of the CM Filter with Circuit Impedance Mismatching

In the traditional filter design, source and load impedances are usually assumed to be 50 Ω. If the effect of parasitic parameters is ignored and impedance matching is assumed, then the ideal insertion loss (IL) curve within 1 kHz–30 MHz has no resonance, as shown in line 1 (solid line) in Fig. 10. However, in the realistic circuit, the parasitic parameters, source impedance, and load impedance change with the frequency. Therefore, the effects of parasitic parameters and impedance should be considered when analyzing the IL of the EMI filter. Line 2 (dashed line) represents the characteristic of IL considering only parasitic parameters, whereas line 3 (dotted line) represents IL considering the parasitic parameters and mismatching impedance.

In Fig. 10, the parasitic parameters may evidently cause resonance in the high-frequency range, which will weaken the attenuation of the EMI filter. Points "A" and "B" represent the resonant points caused by the parasitic parameters of capacitance and inductance, respectively. By comparing lines 2 and 3, a resonant "C" is seen in line 3 at low frequency because line 3 is simulated under the condition of mismatching

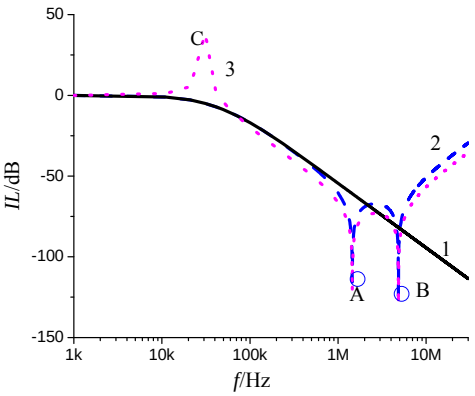

Fig. 10. Effects of parasitic parameters and circuit impedance mismatching state on IL: 1, ideal; 2, only parasitic parameters considered; 3, parasitic parameters and mismatching considered; A, B, and C, resonant points.

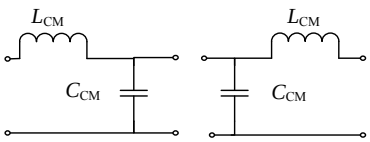

(a) C-L type. (b) L-C type.

Fig. 11. Ideal models of the CM filter.

impedance. Therefore, source and load impedances should be considered when designing the EMI filter.

Based on the previously presented analysis, source and load impedances should be considered when analyzing the IL of the EMI filter. In the realistic circuit, impedance of the converter is usually regarded as the source impedance, which changes with frequency, that is:

$$Z_S = R_S + j\omega L_S + 1/(j\omega C_S), \tag{4}$$

where Z_s represents source impedance, which can be equivalent to a resistance, inductance, and capacitance structure. R_s is the equivalent resistance of the source. Similarly, C_s and L_s represent the equivalent capacitance and inductance of the source, respectively.

In addition, the equivalent impedance of LISN is usually assumed to be 50 Ω. Therefore, load impedance is 25 Ω considering the two CM noise circuits in parallel (Z_L = 25 Ω).

Based on the previously presented analysis of the CM filter, the EMI filter has two kinds, and their ideal models are shown in Fig. 11.

Based on the models of the CM filter shown in Fig. 11, the transmission matrix of the C-L and L-C filters is calculated, which can be expressed as T_{CL} and T_{LC}, respectively, as follows:

$$T_{CL} = \begin{bmatrix} 1 + Z_{LCM}/Z_{CCM} & Z_{LCM} \\ 1/Z_{CCM} & 1 \end{bmatrix}, \tag{5}$$

$$T_{LC} = \begin{bmatrix} 1 & Z_{LCM} \\ 1/Z_{CCM} & 1 + Z_{LCM}/Z_{CCM} \end{bmatrix}, \tag{6}$$

where:

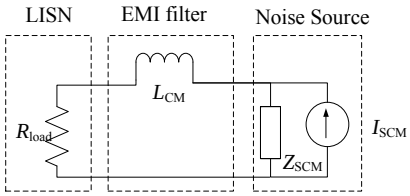

Fig. 12. Test circuit after adding an inductor.

$$Z_{LCM} = \frac{(j\omega L_{CM} + R_m)}{(j\omega L_{CM} + R_m + j\omega C_m)\cdot j\omega C_m}, \tag{7}$$

$$Z_{CCM} = R_m + j\omega L_m + 1/(j\omega C_{CM})\cdot \tag{8}$$

In Equations (7) and (8), Z_{LCM} is the equivalent impedance of CM inductance at high frequency; Z_{CCM} is the equivalent impedance of capacitance at high frequency; R_m is the parasitic resistance of inductance and capacitance; and L_m and C_m are the parasitic inductance and parasitic capacitance, respectively.

Taking the L-C filter as an example, the four parameters of transmission matrix T_{LC} can be expressed as *A*, *B*, *C*, and *D* in Equation (9):

$$T_{LC} = \begin{bmatrix} 1 & Z_{LCM} \\ 1/Z_{CCM} & 1+Z_{LCM}/Z_{CCM} \end{bmatrix} \triangleq \begin{bmatrix} A & B \\ C & D \end{bmatrix}. \tag{9}$$

Therefore, the IL of the L-C filter can be expressed in Equation (10):

$$IL = -20\log\left|\frac{Z_S + Z_L}{AZ_S + B + CZ_SZ_L + DZ_L}\right|. \tag{10}$$

Equation (10) shows that the source impedance (Z_s) has a significant effect on the performance of the EMI filter. Therefore, considering noise impedance when designing the EMI filter is necessary.

Fig. 12 shows the tested circuit assuming that the CM filter is only composed of the inductance.

In the figure, $\bar{V}_1$ and $\bar{V}_2$ denote the voltage of R_{load} before and after linking an inductor, respectively. A_{CM} denotes voltage loss, which can be calculated as follows:

$$\bar{V}_1 = \frac{R_{load}\cdot Z_{SCM}}{R_{load}+Z_{SCM}}\cdot \bar{I}_{SCM}, \tag{11}$$

$$\bar{V}_2 = \frac{R_{load}\cdot Z_{SCM}}{R_{load}+Z_{SCM}+Z_{fCM}}\cdot \bar{I}_{SCM}, \tag{12}$$

$$A_{CM} = \frac{\bar{V}_2}{\bar{V}_1} = 1 + \frac{Z_{LCM}}{R_{load}+Z_{SCM}}, \tag{13}$$

where Z_{SCM} is the source impedance and R_{load} is the impedance of LISN with a value equal to 25 Ω. When $|R_{load}+Z_{SCM}+Z_{fCM}| < |R_{load}+Z_{SCM}|$, the noise of the CM filter may be enlarged.

$$|R_{load}+Z_{SCM}| = \frac{|Z_{fCM}|}{|A_{CM}-1|} \tag{14}$$

According to Equation (14), the amplitude and phase of A_{CM} − 1 are difficult to test. However, $|A_{CM} - 1|$ can be measured easily. Therefore, if $|A_{CM}| >> 1$, then $|A_{CM} - 1|$ can be equal to $|A_{CM}|$. Thus, the maximum and minimum impedances can be obtained as follows:

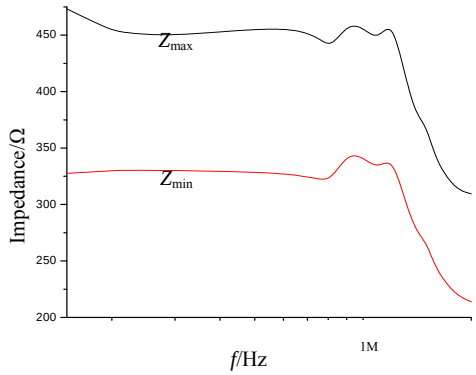

Fig. 13. Frequency characteristics of impedance.

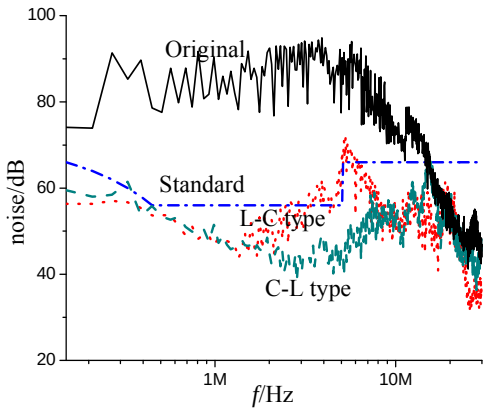

Fig. 14. Noise curve with the CM filter.

$$|Z_{\mathrm{SCM}}|_{\mathrm{Max}} = \left| R_{\mathrm{load}} + \left| \frac{Z_{f\mathrm{CM}}}{A_{\mathrm{CM}}} \right| \right|, \tag{15}$$

$$|Z_{\mathrm{SCM}}|_{\mathrm{Min}} = \left| R_{\mathrm{load}} - \left| \frac{Z_{f\mathrm{CM}}}{A_{\mathrm{CM}}} \right| \right|. \tag{16}$$

According to Equations (15) and (16), the maximum and minimum impedances can be obtained, as shown in Fig. 13.

As presented in the introduction, we can obtain two kinds of CM filters, namely, L-C type and C-L type. Therefore, the characteristics of noise can be tested before and after linking the CM filter, as shown in Fig. 14. The solid line represents original noise, which is far above the noise limit. The dotted line represents noise with the L-C filter, and the dashed line represents noise with the C-L filter. Comparing these two lines, the C-L filter should be adopted, given that attenuation in the C-L type is larger than that in the L-C type, particularly at high frequency. Furthermore, the experiments indicate that the worst case attenuation of the L-C type occurs when noise source impedance is at the maximum. Similarly, the worst case attenuation of the C-L type occurs when noise source impedance is at the minimum. Therefore, in the CM filter design process, the type of CM filter should be selected first and then the filter should be designed according to the worst case attenuation.

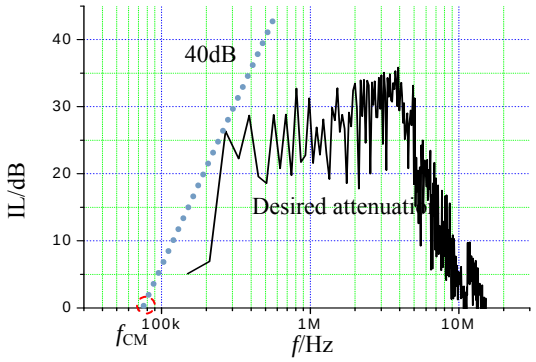

Fig. 15. Desired attenuation.

(a) LC unit. (b) CM and DM capacitor.

Fig. 16. Basic unit of the EMI filter.

Fig. 15 shows how corner frequency f_{CM} can be obtained, in which the desired attenuation indicates the minimum value, which is needed to meet the noise limit requirements; its value can be obtained by subtracting the noise limit from the original noise. In addition, the slope of the dotted line is 40 dB. Thus, f_{CM} can be regarded as the intersection of the dotted line and the horizontal axis.

$$f_{\mathrm{CM}} = \frac{1}{2\pi\sqrt{L_{\mathrm{CM}}C_{\mathrm{CM}}}} \tag{17}$$

IV. Experiments of the Planar EMI Filter

A novel EMI filter prototype is established and experiments are conducted to verify the proposed idea. The basic unit of the EMI filter is shown in Fig. 16.

As shown in Fig. 15, corner frequency is approximately f_{CM} = 75 kHz. For the C-L filter, the worst situation would be that impedance of the noise source is minimal. From Fig. 13, minimal impedance is approximately 326.3 Ω at 150 kHz. Therefore, the impedance of CM inductance at 150 kHz should be smaller than 326.3 Ω to meet the requirements of EMC, and a 300 Ω impedance is selected, which corresponds to inductance of approximately 2 mH, to allot several margins. However, if the phase angle of noise impedance is considered, then inductance must be at least two times of 2 mH. Finally, based on the value of inductance, we can obtain the required CM capacitance of an ideal L-C filter with a value of 12.96 nF.

The structure parameters of the CM and DM capacitors are listed in Table I. Permittivity of the ceramic substrate is approximately 3,000, and the test curves are shown in Fig. 17.

TABLE I
PARAMETERS OF THE CM AND DM CAPACITORS

Layer	Structure size	Quantity/mm
Silver layers	Inside diameter	20.0
	Outside diameter	40.0
	Thickness	1.0
Ceramic substrate	Inside diameter	20.0
	Outside diameter	40.0
	Thickness	1.0

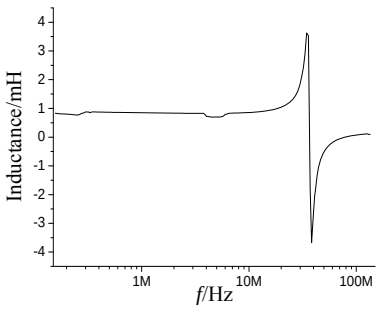

(a) Inductance of the LC unit.

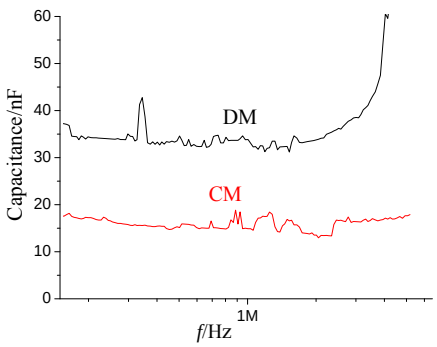

(b) Capacitance of the CM and DM capacitors.

Fig. 17. Parameters of the EMI filter.

According to Fig. 17, inductance and capacitance values of the new EMI filter are not limited by technology and the value of DM capacitance can be increased by the multilayer capacitor units.

As shown in Fig. 17(a), the inductance of the LC unit is approximately 600 μH in the frequency range of 150 kHz to 30 MHz because of the same EMI test frequency range. Then, we can consider the inductance of the LC unit to be 600 μH. Similarly, the capacitance of the CM and DM capacitors is approximately 18 and 37 nF, respectively, in the frequency range of 150 kHz to 6 MHz. In addition, the test results of the capacitance of the DM capacitor would be insignificant because of resonance. In that case, we can consider the DM capacitance of 37 nF and CM capacitance of 18 nF to achieve the purpose of extending DM capacitance.

Figs. 18 and 19 show the proposed prototype of a novel EMI filter and its test circuit, respectively. Fig. 20 shows the corresponding results.

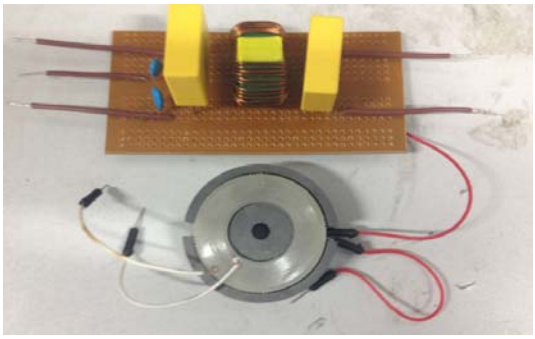

Fig. 18. Prototype of the EMI filter

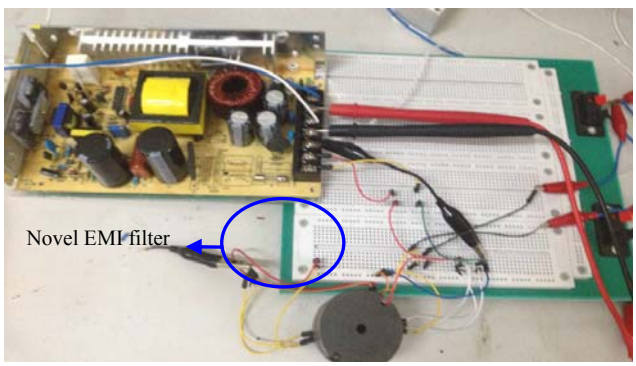

Fig. 19. Test circuit

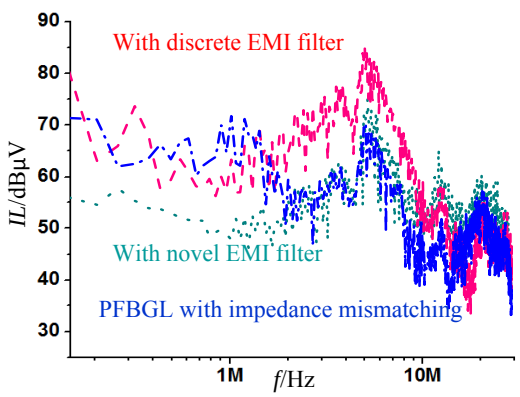

(a) Test result.

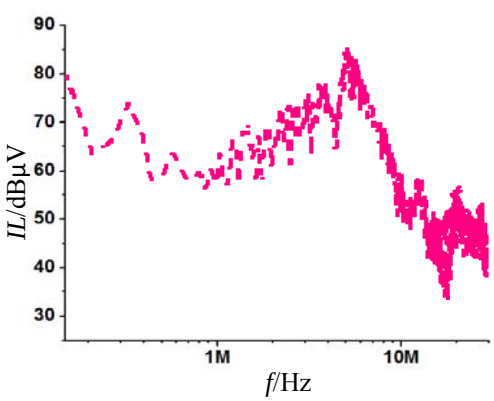

(b) Linkage with the discrete EMI filter.

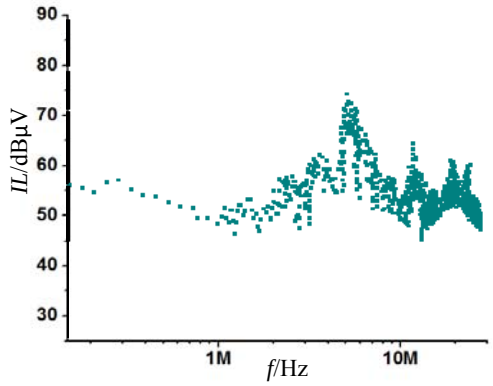

(c) Linkage with the novel EMI filter.

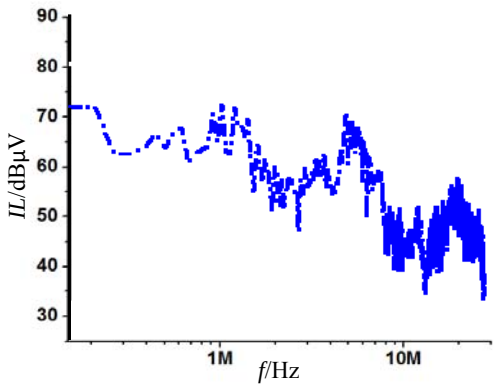

(d) PFBGL with impedance mismatching.

Fig. 20. Noise result after linking with the EMI filter.

In Fig. 20, the dashed line and dashed–dotted line denote the attenuation of the discrete and novel EMI filters, respectively, and the dotted line denotes the attenuation of the novel EMI filter considering impedance mismatching. Furthermore, comparing the dashed line and dashed–dotted line in the figure, the novel EMI filter clearly has better high-frequency characteristics than the discrete EMI filter because the parasitic parameters of the discrete filter are greater. In addition, comparing the dashed–dotted line and dotted line, the novel EMI filter considering impedance mismatching will have better frequency attenuation, given that mismatching of the source and load impedances will affect IL. Therefore, filter structure and source impedance should be considered when designing filters.

V. CONCLUSION

A novel EMI filter is proposed in this study, and the principle of the EMI filter considering impedance mismatching is analyzed. Furthermore, the following conclusions can be drawn:

(1) A type of EMI filter with bi-ground layers is proposed, which allows inductance and capacitance to be designed separately. Compared with the EMI filter with single ground layer, the proposed EMI filter is more feasible and reliable. Specifically, the novel structure has two advantages. First, inductance is not limited by technology, given that the number of spiral wires can be increased significantly in the PCB substrate. Second, capacitance is also not restricted by the area of the spiral wires because of its single-turn structure.

(2) The proposed EMI filter structure can be applied to different source and load impedances without changing the structure. Specifically, for different source and load impedances of CM noise, only the current direction should be changed.

(3) The prototype of the novel EMI filter is established and applied to a small switching power supply. The experimental results verify that the novel structure can suppress noise effectively.

ACKNOWLEDGMENT

This research was supported by the National Natural Science Foundation of China and Education Development Program of Delta Environmental and Educational Foundation. Special thanks are also given to Jiangsu Province University Outstanding Science and Technology Innovation Team Project for the support.

REFERENCES

[1] R. L. Ozenbaugh, *EMI Filter Design*, 2th ed., Marcel Dekker, Inc. Chap.3, pp. 25-65, 2001.

[2] S. Wang, Y. Zhu, X. Zhou, and L. Wu, "Characteristics research for planar common mode EMI filter based on toroidal LC coil," *Transactions of China Electrotechinal Society*, Vol. 26, No. 3, pp. 68-73, Nov. 2011. (in Chinese)

[3] S. Wang and C. Xu, "Design theory and implementation of planar EMI filter based on annular integrated inductor-capacitor unit," *IEEE Trans. Power Electron.*, Vol.28, No.3, pp. 1167-1175, Mar. 2013.

[4] H.-F. Huang and L.-Y. Deng, "Improving the high-frequency performance of integrated EMI filter with multiple ground layers," *Asia-Pacific Symposium on Electromagnetic Compatibility*, pp. 249-252, 2012.

[5] V. Tarateeraseth, K. Y. See, F. G. Canavero, R. W. Chang, "Systematic electromagnetic interference filter design based on information from in-circuit impedance measurements," *IEEE Trans. Electromagn. Compat.*, Vol. 52, No. 3, pp. 588-598, Aug. 2010.

[6] R. Chen, J. D. van Wyk, S. Wang, and W. G. Odendaal, "Planar electromagnetic integrated technologies for integrated EMI filters," *Industry Applications Conference*, Vol. 3, No. 12, pp. 1582-1588, 2003.

[7] X. Wu, D. Xu, Z. Wen, Y. Okuma, and K. Mino, "Design, modeling, and improvement of integrated EMI filter with flexible multilayer foils," *IEEE Trans. Power Electron.*, Vol. 26, No. 5, pp. 1344-1354, May 2011.

[8] S. Ye, "New EMI filter Design Methods for DC-DC and AC-DC Switching Power Supplies," Queen's University, Jun. 2003.

[9] F. Luo, D. Boroyevich, and P. Mattavelli, "Improving EMI filter design with in circuit impedance mismatching,"

Applied Power Electronics Conference and Exposition (APEC), Twenty-Seventh Annual IEEE, pp. 1652-1658, 2012.

[10] J. Espina, J. Balcells, A. Arias, C. Ortega, and N. Berbel, "EMI model of an AC/AC power converter," *Vehicle Power and Propulsion Conference (VPPC)* , pp. 1-6, 2010.

Shishan Wang received his Ph.D. degree from Xi'an Jiaotong University, Xi'an, China in 2003. Since 2004, he has been an Associate Professor with the College of Automation Engineering Nanjing University of Aeronautics and Astronautics, Nanjing, China. His main research interests include electromagnetic compatibility in power electronics system and simulation of multiphysics fields for electrical equipment.

Zheng Song received his B.S. degree in electrical engineering and automation from the Nanjing University of Aeronautics and Astronautics, Nanjing, China in 2013. He is currently working toward his M.S. degree in electrical engineering at the Nanjing University of Aeronautics and Astronautics, Nanjing, China. His main research interests include electromagnetic compatibility of power electronics and design and development of new types of electromagnetic interference filters.

Qianceng Lou received his B.S. degree in applied physics from the Nanjing University of Aeronautics and Astronautics, Nanjing, China in 2015. He is currently working toward his M.S. degree in electrical engineering at the Nanjing University of Aeronautics and Astronautics, Nanjing, China. His main research interests include electromagnetic compatibility of power electronics and design and development of new types of electromagnetic interference filters.